

Analysis of the blowout plasma wakefields produced by drive beams with elliptical symmetry

P. Manwani,* Y. Kang, J. Mann, B. Naranjo, G. Andonian, and J. B. Rosenzweig
Department of Physics and Astronomy, UCLA, Los Angeles, California 90095, USA

(Dated: June 6, 2024)

In the underdense (blowout) regime of plasma wakefield acceleration (PWFA), the particle beam is denser than the plasma. Under these conditions, the plasma electrons are nearly completely rarefacted from the beam channel, resulting in a nominally uniform ion column. Extensive investigations of this interaction assuming axisymmetry have been undertaken. However, the plasma blowout produced by a transversely asymmetric driver possesses quite different characteristics. They create an asymmetric plasma rarefaction region (bubble) which leads to asymmetric focusing in the two transverse planes. This is also accompanied by an undesired non-uniform accelerating gradient. The asymmetric blowout cross-section is found through simulation to be elliptical, and treating it as such permits a simple extension of the symmetric theory. In particular, focusing fields linear in both transverse directions exist in the bubble. The form of the wake potential and the concomitant matching conditions in this elliptical cavity are discussed in this paper. We also discuss bubble boundary estimation in the long driver limit and applications of the asymmetric features of the wakefield.

Plasma wakefield accelerators (PWFA) operate in two main regimes - linear [1] and nonlinear (blowout) [2, 3]. In the blowout case, the strong electric fields of the driver expel the plasma electrons outward, creating a blowout cavity (or bubble) entirely devoid of electrons. The expelled electrons and the electrons within a plasma skin depth of the boundary form a dense electron sheath which envelops the cavity. This plasma electron density and the associated return current shield the driver beam's electromagnetic fields outside of the blowout [2, 4, 5]. While axisymmetric driven scenarios have been extensively studied (see also, *e.g.* [6] and [7]), there are still many open questions to explore in the physics of plasma structures formed by strongly asymmetric drivers [8]. The blowout created by these asymmetric, or flat, beams can be well-approximated by an elliptical cross-sectional form. Subsequently, the potential inside these elliptical, cavities translating at nearly the speed of light, is quadratic, yielding linear transverse electric fields [9, 10]. We use the three-dimensional particle-in-cell (PIC) code OSIRIS [11] to investigate the electromagnetic fields inside the elliptical blowout cavity. We then use these phenomenological results to guide development of a theoretical model.

Throughout this letter we use normalized plasma units, where densities are normalized to the density of the plasma, n_0 , which specifies the electron plasma frequency $\omega_p = \sqrt{n_0 e^2 / m_e \epsilon_0}$. In this scheme the unitless notation is implemented as follows: time is normalized to ω_p^{-1} ; velocities to the speed of light c ; masses to the electron mass m_e ; distance to the plasma skin depth $k_p^{-1} = c / \omega_p$; particle charge to the electron charge magnitude e ; and electromagnetic field amplitudes to the so-termed wave-breaking value $m_e c \omega_p / e$. There are source terms in our model and their corresponding subscripts correspond to:

the ions (i), the plasma electrons (e), and the particle beam (b). Here we assume that the ions are stationary to simplify our analysis. This assumption holds when the focusing phase advance of the ions is small, $\Delta\phi = \sigma_z \sqrt{\pi Z_i n_b / m_i} \ll 1$, where Z_i is the ionization state of the ions, n_b is the beam density, m_i is the mass of the ions and σ_z is the bunch length [12]. This assumption allows us to remove the current due to the plasma ions and assume a constant plasma ion density ($n_i = 1$).

The source terms are then given as: the charge density $\rho = \rho_b + \rho_e + 1$ and the current density $\mathbf{J} = \mathbf{J}_b + \mathbf{J}_e$. The equations of motion for the plasma electrons can be written in Hamiltonian form by introducing the vector and scalar potentials \mathbf{A} and ϕ , and the canonical momenta $\mathbf{P} = \mathbf{p} + \mathbf{A}$ associated with the fields. The beam evolution occurs on a much larger timescale than the evolution of the plasma wakefield in the co-moving frame, permitting use of the quasi-static approximation $(x, y, z, t) \rightarrow (x, y, \xi \equiv t - z, s \equiv z)$, where we assume a slowly-varying disturbance in s , that is $\partial_s \ll \partial_\xi$. Maxwell's equations for the normalized potentials in the Lorentz gauge under this approximation reduce to

$$\nabla_\perp^2 \begin{bmatrix} \phi \\ \mathbf{A} \end{bmatrix} = - \begin{bmatrix} \rho \\ \mathbf{J} \end{bmatrix}, \quad (1)$$

where $\nabla_\perp^2 = \partial_x^2 + \partial_y^2$ is the transverse Laplacian operator. The Lorentz gauge condition $\nabla \cdot \mathbf{A} + \frac{\partial \phi}{\partial t} = 0$ can now be written as $\nabla_\perp \cdot \mathbf{A}_\perp = -\frac{\partial}{\partial \xi} (\phi - A_z) = -\frac{\partial}{\partial \xi} \psi$. Here, $\psi = \phi - A_z$ is the wake potential (or quasi-potential) which obeys the Poisson equation $-\nabla_\perp^2 \psi = \rho - J_z$. The continuity equation in the co-moving coordinate can be written as: $\frac{\partial}{\partial \xi} (\rho - J_z) + \nabla_\perp \cdot \mathbf{J}_\perp$.

In this case, the Hamiltonian is given by $H = \gamma + \phi$ with the Lorentz factor $\gamma = \sqrt{1 + |\mathbf{p}|^2}$. In the quasi-static approximation, the Hamiltonian depends on z and t only in the combination $\xi = t - z$. Hamilton's equations lead to the conservation of $H - P_z$ via: $\frac{dH}{dt} = \frac{\partial H}{\partial t} = -\frac{\partial H}{\partial \xi} =$

* pkmanwani@gmail.com

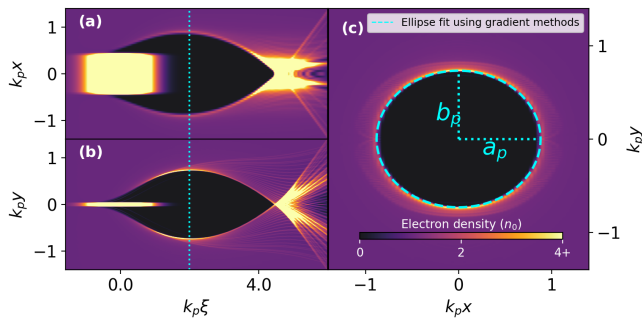


FIG. 1: Plasma wakefield created by a flat top driver with beam density $n_b = 20$, having asymmetric spot sizes: $a = 0.424$, $b = 0.0424$. The longitudinal slices in the X-Z plane (a) and Y-Z plane (b), the transverse slice showing the elliptical profile (c).

$-\frac{\partial H}{\partial z} = \frac{dP_z}{dt}$. If the electrons were initially at rest, this implies, $\gamma + \phi - p_z - A_z = 1$ [13, 14]. After substituting for the wake potential, this equation reduces to

$$\gamma + \psi - p_z = 1 \quad (2)$$

The electromagnetic fields can be found from the potentials:

$$E_z = \frac{\partial \psi}{\partial \xi}; \quad \mathbf{E}_\perp = -\nabla_\perp \phi - \frac{\partial \mathbf{A}_\perp}{\partial \xi} \quad (3)$$

$$\mathbf{B}_\perp = \nabla_\perp \times \mathbf{A}_z + \nabla_z \times \mathbf{A}_\perp; \quad B_z = \nabla_\perp \times \mathbf{A}_\perp$$

Note that when one considers forces on the beam, they are all simply, in the relativistic approximation, derived from ψ . Here we are considering instead the plasma response, and so the scenario of interest is more complex.

Indeed, when the driver interacts with an underdense plasma, plasma electrons are strongly repelled by the first-order Coulomb force due to the beam charge, with magnetic effects becoming important for a relativistic plasma response, as is found in the blowout regime. This repulsion leads to strong, non-laminar plasma motion, which upon evacuation of the plasma electrons from the beam channel ultimately leads to formation of a blowout sheath surrounding a plasma-electron-free cavity.

To proceed with our inquiry into extending the understanding of these plasma dynamics into asymmetric scenarios, we first consult the results of electromagnetic particle-in-cell (PIC) simulations (see Figure 1, which show the output from the code OSIRIS[11]). When considering a transversely elliptical-shaped driver beam, the blowout cavity and sheath (the cavity boundary) also take on elliptical shapes in cross-section. The transverse asymmetry of the wakefield produced by the asymmetric beam can be seen in the longitudinal slices shown in Figure 1. The asymmetry more disperses sheath electron trajectories behind the blowout in a more complex manner, contrasting the symmetric case where the simultaneous crossing of trajectories results in a large transversely-integrated density spike. The transverse slice of the wake-

field itself shows the elliptical cavity cross-section created by the evacuated plasma electrons.

The resulting ellipse semi-major axis a_p and semi-minor axis b_p may be found by numerically evaluating the boundary positions. The values of ellipse dimensions were obtained by a least-squares fitting of select boundary points, with boundary points marking the position maximum gradient of density for 100 radially-directed line searches taken at uniformly spaced angles.

Since the cavity is nearly completely evacuated of the plasma electrons, one can easily obtain the scalar potential due to the remaining ions, $\phi_i(\xi) = -\frac{x^2 b_p(\xi) + y^2 a_p(\xi)}{2(a_p(\xi) + b_p(\xi))}$ [15]. The electron sheath can be well-approximated as infinitesimally thin in this calculation. Indeed, at the boundaries, the plasma electrons exhibit a density well in excess than unity, reducing the nominal plasma skin-depth and partly validating the infinitesimal sheath approximation. We may then proceed without using an external fitting parameter, as was done in Ref. [16]. Additionally, as we assume that no electromagnetic fields exist outside the blowout due to the shielding provided by the sheath at $d\Omega(\xi)$, we may then set the wake potential to be zero everywhere outside the blowout region. Finally, the constant charge density inside the cavity from the ions alone enables us to solve for the wake: $\nabla_\perp^2 \psi(\xi) = -1$, with $\psi|_{a\Omega(\xi)} = 0$. We note the absence of a sheath-dependent term, $\psi_s(x, y, \xi)$, which will be further considered empirically.

We can obtain the solution of the wake potential by switching the analysis to elliptical coordinates:

$$\psi = -\frac{c^2}{8} \left(\cosh 2\mu - \cosh 2\mu_0 + \left(1 - \frac{\cosh 2\mu}{\cosh 2\mu_0} \right) \cos 2\nu \right) \quad (4)$$

Here μ and ν are the elliptical coordinates, and μ_0 and $c = \sqrt{a_p^2 - b_p^2}$ are the elliptical boundaries and focal length of the ellipse, respectively at each value of ξ . Converting the results back to Cartesian coordinates using $x = c \cosh \mu \cos \nu$ and $y = c \sinh \mu \sin \nu$, we find

$$\psi = \frac{a_p^2 b_p^2 - (x^2 b_p^2 + y^2 a_p^2)}{2(a_p^2 + b_p^2)} \quad (5)$$

We note that this wake potential, which determines the motion of ultra-relativistic electrons in the blowout cavity is quadratic in x and y . As this potential thus represents a two-dimensional simple-harmonic oscillator, focal characteristics and thus matched beam conditions in both transverse planes can be derived from Eq. 5. In general, the wakefields can be derived from the gradient

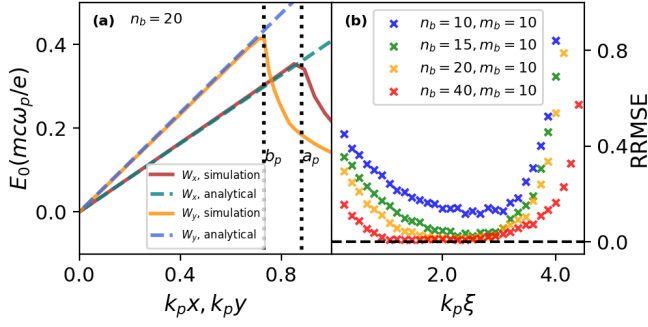


FIG. 2: Short beam ($\sigma_z = 0.5$) driver, where corresponding to the case of Fig. 1. (a) Transverse wakefield line-outs of the wake, (b) Relative Root Mean Squared Error (RRMSE) between the analytical transverse wakefield W_\perp from different n_b , calculated using the fitted blowout boundary.

of the wake potential, as

$$\begin{aligned}
 W_x &= E_x - B_y = -\frac{\partial\psi}{\partial x} = \frac{b_p^2 x}{a_p^2 + b_p^2} = \frac{x}{1 + \alpha_p^2} \\
 W_y &= E_y + B_x = -\frac{\partial\psi}{\partial y} = \frac{a_p^2 y}{a_p^2 + b_p^2} = \frac{\alpha_p^2 y}{1 + \alpha_p^2} \\
 W_z &= E_{z,p} = \frac{\partial\psi}{\partial\xi} = \frac{a_p b_p}{(a_p^2 + b_p^2)^2} \left((x^2 - y^2 + b_p^2) b_p \frac{\partial a_p}{\partial\xi} \right. \\
 &\quad \left. + (-x^2 + y^2 + a_p^2) a_p \frac{\partial b_p}{\partial\xi} \right)
 \end{aligned} \tag{6}$$

Here $\alpha_p = a_p/b_p$ represents the ellipticity of the plasma blowout at a longitudinal position. Note the linearity of the transverse wakefields in their coordinate. The relative root mean square error (RRMSE) between the fields predicted by an elliptical fit to the sheath, in combination with the above equations (x_i) and the PIC simulated transverse fields (\hat{x}_i), is shown in Figure 2 and is calculated by considering each data point within the blowout boundary: $\text{RRMSE} = \sqrt{\sum_{i=1}^n (x_i - \hat{x}_i)^2 / \sum_{i=1}^n (\hat{x}_i^2)}$. This illustrates that our prediction for the transverse wakes using the elliptical model coincides well with simulations.

While this is not a main thrust of the current work, a few comments on the longitudinal wake W_z are in order. The Panofsky-Wenzel theorem [17] as applied to plasma wakefields follows from their description in terms of a unique potential ψ , that is $\nabla_\perp W_z = \partial_\xi W_\perp$. In the case of a symmetric blowout, W_z has been long known to be independent of x and y . as a result of the constant nature of W_\perp after blowout. With the elliptical shape, this conclusion changes only slightly, due to the possible change in the ellipticity with ξ . We therefore conclude that W_z is weakly dependent on x and y , and in the case that the ellipticity is unchanging in ξ (*i.e.* in the long beam limit, see below), the effect is ignorable. In the short-

beam limit example that we have shown in Figure 2, we cannot robustly determine the evolution of the potential during the initiation of the blowout, and so predictions of $W_z(\xi)$ do not converge to simulations in this region, resulting in a cumulative error due to the absence of the sheath potential, ψ_s .

We now move to the estimation of the elliptical boundaries using the beam parameters in the long beam limit ($r_\perp \ll \gamma\sigma_z$), where we neglect the longitudinal variation of the fields near the axial center of the beam ($\partial_\xi \ll \partial_\perp$). We can obtain the force on the plasma electrons at a position near the sheath, \mathbf{r} , by considering the plasma electron's transverse velocity $\mathbf{v}_\perp = d\mathbf{r}_\perp/dt = (1 - v_z) d\mathbf{r}_\perp/d\xi = (1 + \psi) d\mathbf{r}_\perp/d\xi$, and Eq. 2:

$$\mathbf{F}_\perp = (1 - v_z) \frac{d\mathbf{p}_\perp}{d\xi} = \frac{1}{\bar{\gamma}} (1 + \psi) \frac{d}{d\xi} \left((1 + \psi) \frac{d}{d\xi} \mathbf{r}_\perp \right) \tag{7}$$

$$\mathbf{F}_\perp|_{d\Omega} = \frac{1}{\bar{\gamma}} \left(\frac{d\psi}{d\xi} \frac{d\mathbf{r}_\perp}{d\xi} + \frac{d^2\mathbf{r}_\perp}{d\xi^2} \right) |_{d\Omega} = 0 \tag{8}$$

Neglecting variation ξ allows us to assume transverse forces balance at the boundaries. We additionally assume that the plasma electron longitudinal velocity v_z does not depend on the transverse coordinate. This facilitates the solution to the above equations by providing a linear relationship between ϕ_e and A_e , to which we can add v_z effects as a correction. Using Eq. 3 to convert to a potential description and assuming $v_b = 1$:

$$\begin{aligned}
 \mathbf{F}_\perp &= \nabla_\perp \phi_i + \nabla_\perp \phi_e + \nabla_\perp \phi_b \\
 &\quad + \partial_\xi \mathbf{A}_\perp + (\nabla_\perp \mathbf{A}) \cdot \mathbf{v} - (\mathbf{v} \cdot \nabla) \mathbf{A}_\perp
 \end{aligned} \tag{9}$$

With Eq. 8 and neglecting the longitudinal variation of the transverse velocity and fields leads to the relation:

$$(1 + v_z) \nabla_\perp \psi|_{d\Omega} - v_z \nabla_\perp \phi_i|_{d\Omega} + (1 - v_z) \nabla_\perp \phi_b|_{d\Omega} = 0 \tag{10}$$

We first neglect v_z to get the zero-th order equation in the electrostatic limit. Using Ampere's law in integral form: $\oint \mathbf{B} \cdot d\mathbf{l} = \int (\mathbf{J} + \epsilon_0 \frac{\partial \mathbf{E}}{\partial t}) \cdot d\mathbf{a}$, we can integrate over the transverse plane to remove the left hand side term to get: $I_{z,beam} + I_{z,elec} + \int_0^\infty \frac{\partial^2 \psi}{\partial \xi^2} da = 0$. In the limit of a long beam, the integral term becomes negligible. Consequently, this verifies the equivalence between the return beam current and the plasma return current. The return current layer is located in the electron sheath and the surrounding by the plasma skin-depth k_p^{-1} . By assuming the longitudinal velocity v_z to be constant across this region area, we find that $v_z = \frac{\lambda_b}{\pi(a_p+1)(b_p+1)}$, where λ_b is the beam charge per unit length. This enables us to re-incorporate electromagnetic features, beyond the zero-th order analysis above, in weak blowout scenarios. However, for highly nonlinear blowouts, a comprehensive treatment of the wakefields becomes important.

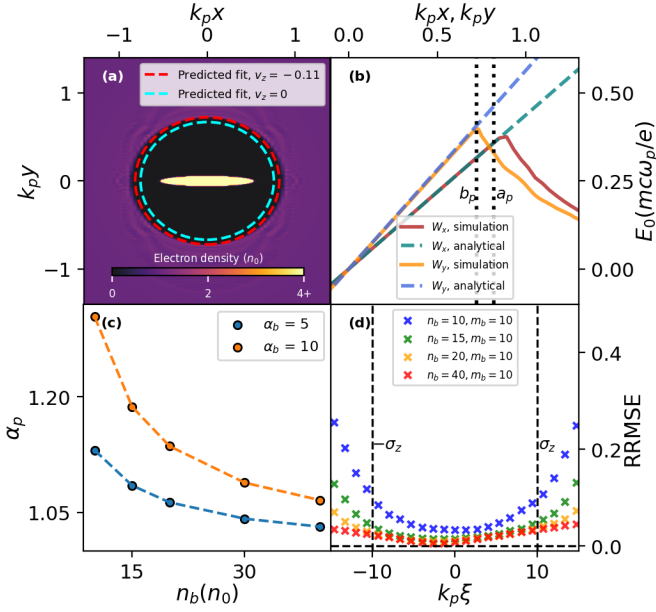


FIG. 3: Long beam ($\sigma_z = 10$) driver: (a) Analytical calculation for the blowout shape using a beam with $n_b = 20$, $a = 0.5$ and $b = 0.05$. (b) Transverse wakefield lineouts of the wake, calculated using the predicted blowout boundary, (c) predicted blowout ellipticity at the center of wake vs beam density and beam ellipticity, (d) Relative Root Mean Squared Error (RRMSE) between the analytically calculated transverse wakefield and the simulation result.

Fortunately, in this limit, axi-symmetry is inherently approached and additional treatment of the higher order moments is not essential.

We use the electric fields of the elliptical driver beam [18] to simultaneously find ψ and the elliptical semi-axes a_p and b_p such that the transverse forces on the ellipse boundaries are minimized. We verify our results by calculating the blowout shape for a long beam driver, predicting the transverse fields and calculating the RRMSE values in Fig. 3 (see Supplemental Material for the details on PIC simulations [19]). The equations that govern the transverse beam dynamics inside the blowout cavity are:

$$x''(z) + K_x x(z) = 0; \quad y''(z) + K_y y(z) = 0 \quad (11)$$

$$K_x = K_r \frac{2}{1 + \alpha_p^2}; \quad K_y = K_r \frac{2\alpha_p^2}{(1 + \alpha_p^2)} \quad (12)$$

where, $K_r = n_p / 2\gamma$ arises from the linear focusing strength of the ions in an axisymmetric ion column, n_p represents the normalized plasma density. The matching conditions of a beam propagating in this blowout cavity are then given as:

$$\sigma_{m,\eta} = \sqrt{\frac{\sqrt{K_\nu^{-1}} \epsilon_{n,\eta}}{\gamma}} \quad (13)$$

where $\eta \in \{x, y\}$ and $\epsilon_{n,\eta}$ are the normalized emittances. The aspect ratio of the matched beam is now determined by the combination of the emittance ratio and the ellipticity of the wake:

$$\frac{\sigma_{m,x}}{\sigma_{m,y}} = \sqrt{\frac{\epsilon_{n,x}}{\epsilon_{n,y}}} \alpha_p \quad (14)$$

The asymmetric focusing fields of the wake provide a route to asymmetric plasma lenses that offer much higher gradients than conventional focusing systems. This could be used in colliders by using low energy drivers to asymmetrically focus a witness beam, which can be used to reduce beamstrahlung [20] at the interaction point, without sacrificing peak luminosity.

$$f_\eta = \frac{1}{K_\eta L} \quad (15)$$

$$z_{w,\eta} = \frac{K_\eta L \beta_{0,\eta} + \alpha_{0,\eta} - L \gamma_{0,\eta}}{K_\eta^2 L^2 \beta_{0,\eta} + 2K_\eta L \alpha_{0,\eta} + \gamma_{0,\eta}} \quad (16)$$

where, L is the length of the plasma lens, $[\alpha_{0,\eta}, \beta_{0,\eta}, \gamma_{0,\eta}]$ are the Courant-Snyder parameters [21] of the beam at the entrance of the plasma, f_η represents the focal lengths of the thin plasma lens and $z_{w,\eta}$ is the location of the beam waist for the η axis under the assumption that we are in the thin lens regime and that the phase advance is small ($\Delta\phi_l = \int_0^L 1/\beta(z) \ll 1$) [22]. For the same initial Courant-Snyder parameters in both transverse directions, there exist multiple solutions for $z_{w,x} = z_{w,y}$. The corresponding equation is cubic, leading to lengthy, albeit closed, forms. More concisely, we may solve for the lens length:

$$L = \beta \frac{(\alpha + f_x^{-1}\beta)(\alpha + f_y^{-1}\beta) - 1}{(1 + \alpha^2)(2\alpha + (f_x^{-1} + f_y^{-1})\beta)} \quad (17)$$

where $\alpha = \alpha_{0,\eta}$, $\beta = \beta_{0,\eta}$, $f_x^{-1} = K_x L$ and $f_y^{-1} = K_y L$ are the x and y inverse focal lengths, and we have used $\gamma_0 = (1 + \alpha_0^2)/\beta_0$. This allows us to remove the astigmatism that could be introduced by the asymmetry, while retaining the asymmetric ratio in the focusing terms. The final aspect ratio of the spot sizes ($\sigma_{x,f}/\sigma_{y,f}$) can be calculated and is given by:

$$\frac{\sigma_{x,f}}{\sigma_{y,f}} = \sqrt{\frac{\epsilon_{n,x} \alpha_0^2 + \beta_0 K_x \alpha_p^2 L (2\alpha_0 + \beta_0 K_x \alpha_p^2 L) + 1}{\epsilon_{n,y} (\alpha_0 + \beta_0 K_x L)^2 + 1}} \quad (18)$$

TABLE I: Table of parameters for the simulation shown in Figure 4.

Parameter	Driver (Witness)
Total beam charge, Q_b	1.5 (0.5) nC
Beam energy, E_b	10 (10) GeV
Bunch length, σ_z	10 (5) μm
Beta function, $\beta_{0,x}, \beta_{0,y}$	20, 0.2 (4, 4) cm
Energy spread	0.1%
Normalized emittance, $\epsilon_{n_x}, \epsilon_{n_y}$	3,3 (3,3) $\mu\text{m-rad}$
Plasma density, n_0	$3 \times 10^{16} \text{ cm}^{-3}$
Plasma particles per cell	4

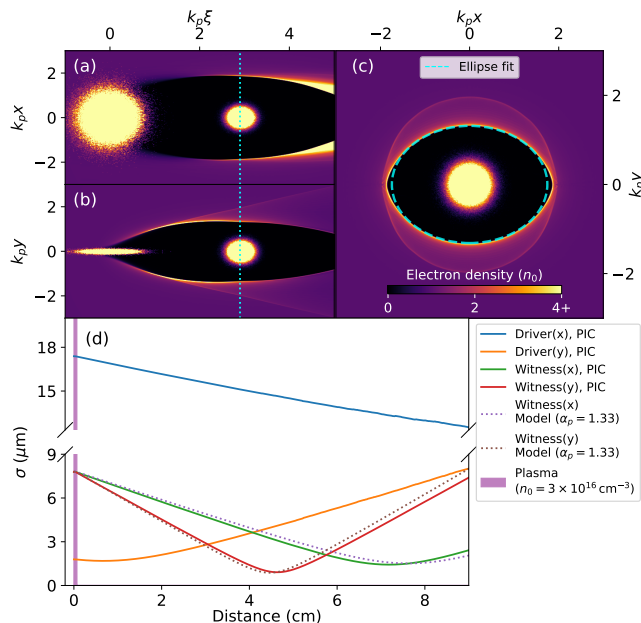


FIG. 4: Asymmetric focusing using an asymmetric driver and axisymmetric witness beam. The top figure represents the longitudinal slices, (a) X-Z and (b) Y-Z, showing the witness beam position ($\xi = 2.9$), and the transverse slice at that position (c). The bottom figure (d) shows the predicted (dotted) and the simulated (solid) result for the two beams after the asymmetric focusing kick introduced by the plasma lens.

The asymmetric phase advance in the two directions can be leveraged by employing a thicker lens to increase the final beam asymmetry at the interaction point. To preserve the transverse emittance of a beam propagating into the plasma, an adiabatic plasma is typically used, which is created by ensuring that the plasma density changes slowly compared to the length scale of the beam's betatron oscillations, $\frac{1}{2} \left| \frac{d\beta_m}{dz} \right| \ll 1$, where $\beta_{m,\eta} = \sqrt{1/K_\eta}$ [23]. However, in asymmetric scenarios where focusing relies on ellipticity, the adiabaticity condition changes as follows:

$$\begin{aligned}
 X : \frac{\beta_{mx}}{4} \left| -\frac{1}{n_p} \frac{dn_p}{dz} + \frac{2\alpha_p}{(1+\alpha_p^2)} \frac{d\alpha_p}{dz} \right| &\ll 1 \\
 Y : \frac{\beta_{my}}{4} \left| -\frac{1}{n_p} \frac{dn_p}{dz} + \frac{2}{\alpha_p(1+\alpha_p^2)} \frac{d\alpha_p}{dz} \right| &\ll 1
 \end{aligned}
 \tag{19}$$

The asymmetric plasma lens experiment can be conducted at FACET-II as part of the thin plasma lens experiment [24]. The asymmetric driver can be created using conventional focusing systems, creating an asymmetric blowout in the plasma jet. The asymmetry of the focusing fields can be controlled by varying the charge and the aspect ratio of the driver beam. These fields may then provide an asymmetric focusing kick to a co-propagating witness beam. This experiment has the potential of corroborating the findings outlined in this paper and we investigate this scenario (parameters shown in Table I) using QuickPIC, a 3D quasi-static PIC code [25]. The results along with the predictions using the elliptical model are shown in Figure 4, where the ellipticity is calculated from fitting an ellipse to the plasma wake at the longitudinal position corresponding to the center of the witness beam. The blowout produced by a Gaussian beam has a wider sheath, thereby decreasing ellipticity and consequently diminishing the asymmetry in the focusing fields. This warrants further investigation of the effects of the sheath, and will be the topic of another paper [26].

In this paper, we have created a phenomenological model for understanding the structure of plasma columns formed by elliptical beams which is crucial as it dictates the focusing forces of the wakefield, thus influencing beam dynamics significantly. This comprehension is essential for plasma wakefield experiments and scenarios involving plasma afterburners utilizing asymmetric beams. The findings presented herein shed light on the ellipticity and emittance requirements for achieving beam matching within the elliptical blowout cavity. The disparity in focusing forces in the two transverse planes presents innovative prospects, including the development of an asymmetric plasma lens and a plasma wakefield experiment planned at the Argonne Wakefield Accelerator (AWA) using a beam with asymmetric transverse emittances [27, 28], where we can use the results shown here, to match the driver to the plasma wakefield. We have listed additional comparisons in the Supplemental material [19]. While this paper lays the foundation, further research is necessary to fully characterize asymmetric wakefields as was done for axisymmetric beams in [4, 16] and ongoing efforts aim to generalize properties of this asymmetric beam-plasma interaction.

The authors would like to thank N. Majernik for insightful discussions. This work was performed with the support of the US Department of Energy under Contract No. DE-SC0017648 and DE0SC0009914. This work used resources of the National Energy Research Scientific Computing Center (NERSC), a U.S. DOE Office of

-
- [1] P. Chen, J. M. Dawson, R. W. Huff, and T. Katsouleas, Acceleration of electrons by the interaction of a bunched electron beam with a plasma, *Phys. Rev. Lett.* **54**, 693 (1985).
- [2] J. B. Rosenzweig, B. Breizman, T. Katsouleas, and J. J. Su, Acceleration and focusing of electrons in two-dimensional nonlinear plasma wake fields, *Phys. Rev. A* **44**, R6189 (1991).
- [3] N. Barov, J. B. Rosenzweig, M. E. Conde, W. Gai, and J. G. Power, Observation of plasma wakefield acceleration in the underdense regime, *Phys. Rev. ST Accel. Beams* **3**, 011301 (2000).
- [4] W. Lu, C. Huang, M. Zhou, W. B. Mori, and T. Katsouleas, Nonlinear theory for relativistic plasma wakefields in the blowout regime, *Phys. Rev. Lett.* **96**, 165002 (2006).
- [5] S. A. Yi, V. Khudik, C. Siemon, and G. Shvets, Analytic model of electromagnetic fields around a plasma bubble in the blow-out regime, *Physics of Plasmas* **20**, 013108 (2013), https://pubs.aip.org/aip/pop/article-pdf/doi/10.1063/1.4775774/13429408/013108_1.online.pdf.
- [6] N. Barov, J. B. Rosenzweig, M. C. Thompson, and R. B. Yoder, Energy loss of a high-charge bunched electron beam in plasma: Analysis, *Phys. Rev. ST Accel. Beams* **7**, 061301 (2004).
- [7] J. B. Rosenzweig, N. Barov, M. C. Thompson, and R. B. Yoder, Energy loss of a high charge bunched electron beam in plasma: Simulations, scaling, and accelerating wakefields, *Phys. Rev. ST Accel. Beams* **7**, 061302 (2004).
- [8] S. S. Baturin, Flat bubble regime and laminar plasma flow in a plasma wakefield accelerator, *Phys. Rev. Accel. Beams* **25**, 081301 (2022).
- [9] P. Manwani *et al.*, Beam Matching in an Elliptical Plasma Blowout Driven by Highly Asymmetric Flat Beams, in *Proc. IPAC'22*, International Particle Accelerator Conference No. 13 (JACoW Publishing, Geneva, Switzerland, 2022) pp. 1802–1805.
- [10] P. Manwani, N. Majernik, J. Mann, Y. Kang, D. Chow, H. Ancelin, G. Andonian, and J. Rosenzweig, Flat beam plasma wakefield accelerator (2023), [arXiv:2305.01902](https://arxiv.org/abs/2305.01902) [physics.acc-ph].
- [11] R. A. Fonseca, S. F. Martins, L. O. Silva, J. W. Tonge, F. S. Tsung, and W. B. Mori, One-to-one direct modeling of experiments and astrophysical scenarios: pushing the envelope on kinetic plasma simulations, *Plasma Physics and Controlled Fusion* **50**, 124034 (2008).
- [12] J. B. Rosenzweig, A. M. Cook, A. Scott, M. C. Thompson, and R. B. Yoder, Effects of ion motion in intense beam-driven plasma wakefield accelerators, *Phys. Rev. Lett.* **95**, 195002 (2005).
- [13] P. Mora and T. M. Antonsen, Jr., Kinetic modeling of intense, short laser pulses propagating in tenuous plasmas, *Physics of Plasmas* **4**, 217 (1997), https://pubs.aip.org/aip/pop/article-pdf/4/1/217/12532941/217_1.online.pdf.
- [14] W. Lu, C. Huang, M. Zhou, M. Tzoufras, F. S. Tsung, W. B. Mori, and T. Katsouleas, A nonlinear theory for multidimensional relativistic plasma wave wakefields), *Physics of Plasmas* **13**, 056709 (2006), https://pubs.aip.org/aip/pop/article-pdf/doi/10.1063/1.2203364/15804477/056709_1.online.pdf.
- [15] M. R. Shubaly, Space charge fields of elliptically symmetrical beams, *Nuclear Instruments and Methods* **130**, 19 (1975).
- [16] A. Golovanov, I. Y. Kostyukov, A. Pukhov, and V. Malka, Energy-conserving theory of the blowout regime of plasma wakefield, *Phys. Rev. Lett.* **130**, 105001 (2023).
- [17] W. K. H. Panofsky and W. A. Wenzel, Some Considerations Concerning the Transverse Deflection of Charged Particles in Radio-Frequency Fields, *Review of Scientific Instruments* **27**, 967 (1956), https://pubs.aip.org/aip/rsi/article-pdf/27/11/967/19098135/967_1.online.pdf.
- [18] G. Parzen, Electric fields of a uniformly charged elliptical beam (2001), [arXiv:physics/0108040](https://arxiv.org/abs/physics/0108040) [physics.acc-ph].
- [19] See supplemental material at [url will be inserted by publisher] for details on pic simulations and computational methods.
- [20] P. Chen, Differential luminosity under multiphoton beamstrahlung, *Phys. Rev. D* **46**, 1186 (1992).
- [21] E. Courant and H. Snyder, Theory of the alternating-gradient synchrotron, *Annals of Physics* **3**, 1 (1958).
- [22] J. B. Rosenzweig and P. Chen, Beam optics of a self-focusing plasma lens, *Phys. Rev. D* **39**, 2039 (1989).
- [23] M. D. Litos, R. Ariniello, C. E. Doss, K. Hunt-Stone, and J. R. Cary, Beam emittance preservation using gaussian density ramps in a beam-driven plasma wakefield accelerator, *Philosophical Transactions of the Royal Society. A, Mathematical, Physical and Engineering Sciences* **377**, 10.1098/rsta.2018.0181 (2019).
- [24] C. E. Doss, E. Adli, R. Ariniello, J. Cary, S. Corde, B. Hidding, M. J. Hogan, K. Hunt-Stone, C. Joshi, K. A. Marsh, J. B. Rosenzweig, N. Vafaei-Najafabadi, V. Yakimenko, and M. Litos, Laser-ionized, beam-driven, underdense, passive thin plasma lens, *Phys. Rev. Accel. Beams* **22**, 111001 (2019).
- [25] C. Huang, V. Decyk, C. Ren, M. Zhou, W. Lu, W. Mori, J. Cooley, T. Antonsen, and T. Katsouleas, Quickpic: A highly efficient particle-in-cell code for modeling wakefield acceleration in plasmas, *Journal of Computational Physics* **217**, 658 (2006).
- [26] P. Manwani, Y. Kang, G. Andonian, J. Rosenzweig, and J. Mann, Comparison of flat beam pwfa analytic model with pic simulations (), presented at IPAC'24, Nashville, TN, USA, May 2024, paper MOPR65, unpublished.
- [27] T. Xu, M. Conde, G. Ha, M. Kuriki, P. Piot, J. Power, and E. Wisniewski, Generation High-Charge of Flat Beams at the Argonne Wakefield Accelerator, in *10th International Particle Accelerator Conference* (2019).
- [28] P. Manwani *et al.*, Asymmetric Beam Driven Plasma Wakefields at the AWA, in *Proc. IPAC'21* (JACoW Publishing, Geneva, Switzerland) pp. 1732–1735.